Mitotic partitioning of endosomes and lysosomes

Trygve Bergeland, Jannicke Widerberg, Oddmund Bakke and Tommy W. Nordeng

Background: Some of the mechanisms underlying cell division and partitioning of the cellular components into the daughter cells are well known. Within the endomembrane system, there is a general cessation of membrane traffic, including endocytosis and endosome fusion, at the onset of mitosis. However, the fate of endosomes and lysosomes during mitosis has been less well studied.

Results: Using video and confocal microscopy of living cells, we show here that endosomes and lysosomes remain intact and separate during mitosis. The segregation into daughter cells takes place by coordinated movements, and during cytokinesis, these organelles accumulate in the vicinity of the microtubule organization center. However, partitioning into daughter cells is not more accurate than a calculated stochastic distribution, despite the apparent order to the process.

Conclusion: We conclude that partitioning of endosomes and lysosomes is an ordered, yet imprecise, process, and that the organelle copy number is maintained by the daughter cells.

Address: Division of Molecular Cell Biology, Department of Biology, University of Oslo, Oslo, Norway.

Correspondence: Oddmund Bakke
E-mail: oddmund.bakke@bio.uio.no

Received: **8 February 2001**
Revised: **8 March 2001**
Accepted: **9 March 2001**

Published: **1 May 2001**

Current Biology 2001, 11:644–651

0960-9822/01/$ – see front matter

Introduction

During mitosis, the biosynthetic activity in animal cells is slowed down, and the main task is then to segregate the chromosomes and to partition all other cellular components to the two daughter cells. Cellular organelles are partitioned into daughter cells by more or less stringent mechanisms. The most ordered partitioning is based on the mitotic spindle [1]. This insures highly accurate segregation of chromosomes by tethering each sister chromatid to one or the other of the spindle poles through microtubules attached to the kinetochores. When partitioning is not directed, the distribution is random, based on the laws of probability [2]. In this case, the accuracy of partitioning depends on the number of organelles, a uniform distribution, and an equal division of the cell's volume into the nascent daughter cells.

In most eukaryotic cells, the onset of mitotic prophase is marked by significant changes in organelle structure and function. Some organelles fragment and vesiculate, a mechanism that facilitates the partitioning between daughter cells (for a review, see [2]). The mechanisms underlying organelle fragmentation involve a transient inhibition of fusion machinery in the face of the continuing budding of transport vesicles, and the result is a progressive vesiculation of the organelles. The Golgi complex provides a striking example of membrane redistribution, although there is still some controversy about the precise mechanisms involved in this process (for a review, see [3]). During mitosis, the Golgi apparatus breaks down from a single copy organelle into several vesicle clusters. It has been suggested that there are a stereotypical number of vesicle clusters that are partitioned to the daughter cells by an ordered and accurate mechanism [4], possibly due to interactions with the mitotic spindle microtubules [5].

The fate of endosomes and lysosomes during cell division has not been revealed in detail thus far, most likely because of the dynamic properties of these organelles. Endosomes have been shown to exist both as distinct organelles and in an interconnected network [6, 7]. Lysosomes are also dynamic, but mostly distinct, and more than 1000 organelles per cell have been recorded [8, 9]. The lysosome equivalent in fungi is the vacuole. In budding yeast, there are often only 1–5 vacuoles, and these are inherited by an ordered mechanism that does not involve fragmentation [10].

By using confocal and video microscopy, we have described the partitioning of endosomal and lysosomal populations labeled with endocytosed fluorochromes or a GFP-tagged early endosomal marker. Moreover, we utilized the enlarged endosomes induced by overexpression of invariant chain to study the inheritance of a particular endosome in more detail.

Results

Endosomal and lysosomal populations remain distinct during cell division

To label late endocytic compartments, MDCK cells were incubated with BSA-Alexa 594 overnight and washed and incubated with microscopy medium without BSA-Alexa

Figure 1

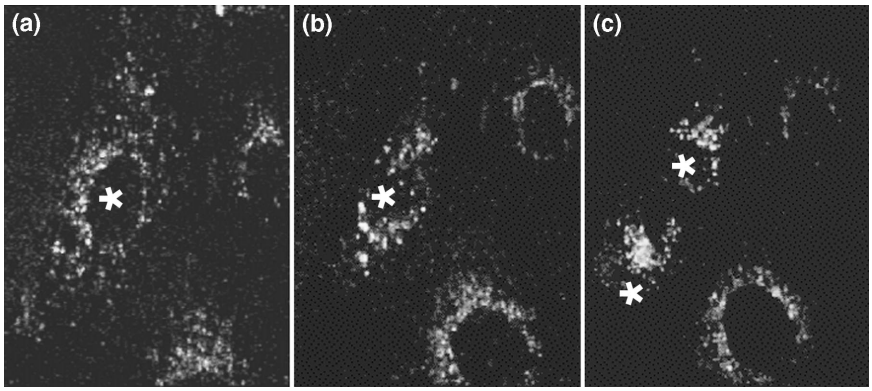

Segregation of late endosomes and lysosomes. To label late endocytic compartments, cells were incubated overnight with BSA-Alexa 594 and then chased for 30 min in medium without BSA-Alexa 594. Confocal microscopy images of live cells at 37°C were acquired. An asterisk identifies **(a)** the mother cell 45 min before division, **(b)** the mother cell during mitosis, and **(c)** the daughter cells 45 min after division (supplementary movie 1, image every min).

594 for at least 30 more minutes. Images were acquired every 5 min and show that late endocytic compartments remained labeled with BSA-Alexa 594 during cell division (Figure 1). To study the fate of early endosomes during mitosis, we used cells that were stably transfected with EEA1-GFP. At the onset of mitosis, the cytoplasmic fluorescence by EEA1-GFP increased, and this was maintained throughout mitosis until it decreased in the newly formed daughter cells (Figure 2). However, endosomes were still labeled, indicating a shift toward free EEA1 in mitosis. To exclude that this observation was an artifact of the more globular shape of mitotic cells, the MDCK cells were treated with trypsin, but the resulting globular shape did not result in similar observations (data not shown).

To study the intracellular distribution of endosomes and lysosomes in detail, we performed two-color time-lapse experiments in which two-channel images of five confocal planes were acquired every minute and merged to one plane. Digital analysis of high-resolution confocal microscopy images showed that average interphase MDCK II cells contained about 400 early endosomes (EEA1-GFP-positive) and about 800 late endocytic compartments (BSA-Alexa 594-positive). In interphase cells, there was very little overlap between BSA-Alexa 594 chased for 30

Figure 2

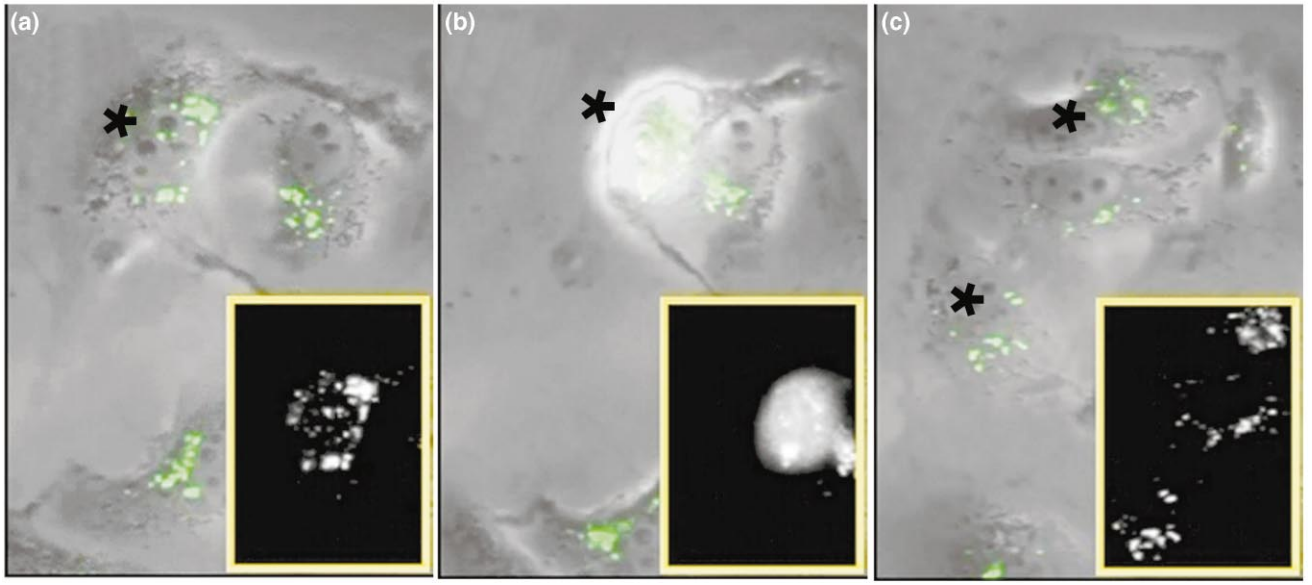

Distribution of EEA1-GFP during mitosis. Live dividing cells at 37°C were monitored by phase contrast and video fluorescence microscopy. EEA1-GFP labeling is displayed as green (big window) or grayscale (small frame). An asterisk identifies **(a)** the mother cell 60 min before division, **(b)** the mother cell during mitosis, and **(c)** the daughter cells 60 min after division (supplementary movie 2, image every 20 min).

Figure 3

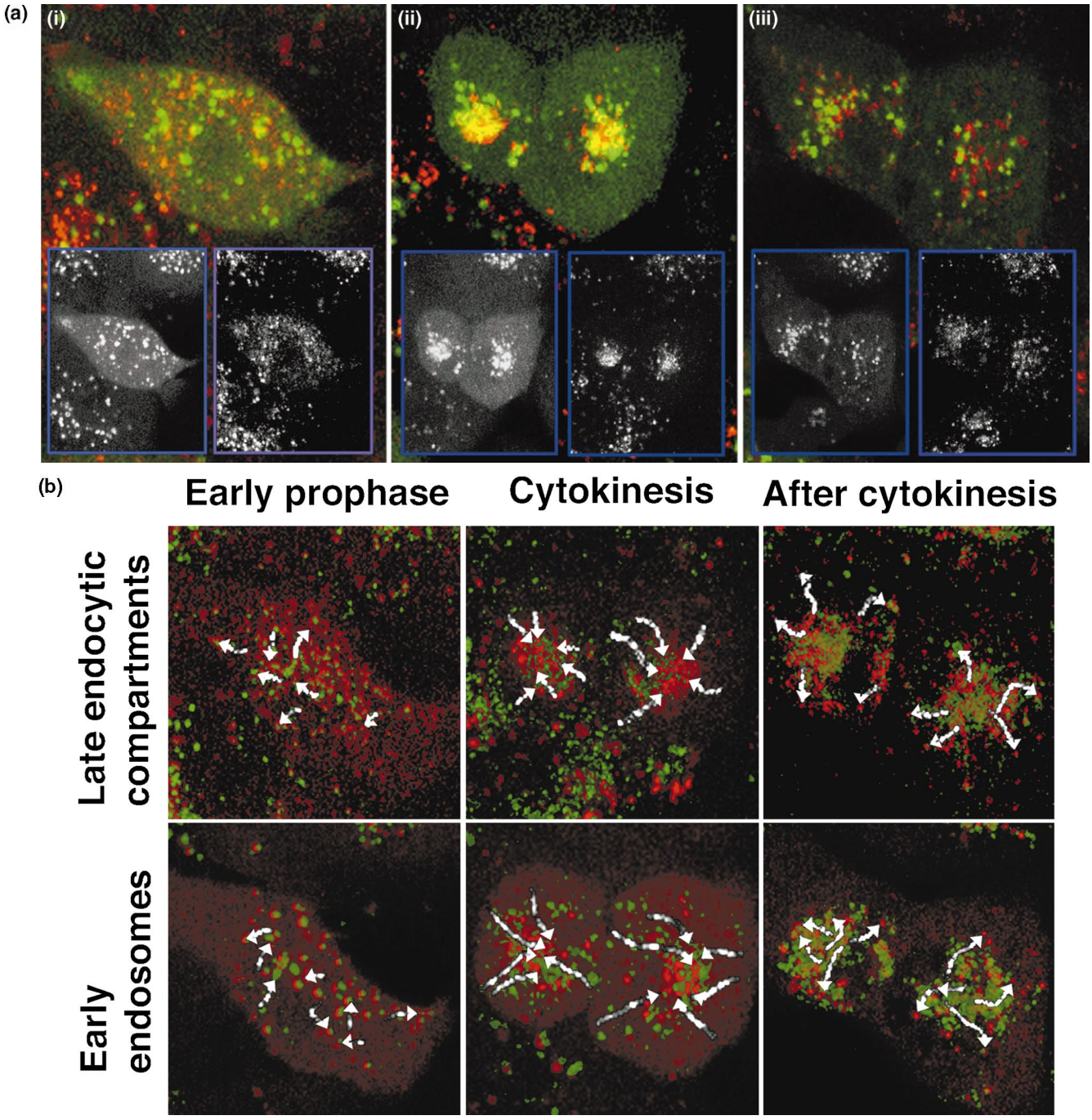

Simultaneously labeled endosomes and lysosomes during mitosis. MDCK cells expressing EEA1-GFP were incubated overnight with BSA-Alexa 594 and chased to label late endocytic compartments. Live, dividing cells at 37°C were studied by dual-parameter confocal microscopy. Five different z scans were acquired every minute and merged. **(a)** Each micrograph displays a two-channel overlay (big frame) and separate grayscale images of EEA1-GFP labeling (left small frame) and BSA-Alexa 594 (right small frame) of (i) cells entering mitosis, (ii) 2 min after cytokinesis, and (iii) 30 min after cytokinesis. **(b)** Between six and ten images from different parts of the image sequences were selected. Image subtraction was performed to visualize changes during each sequence. The second image in a sequence was subtracted from the first, the third from the second, and so on. The subtracted images were merged and displayed (green channel). To identify vesicle movements, subtracted images were analyzed individually. The pattern of movement of selected vesicles is labeled in white; the arrowheads indicate the direction. The red channel displays the final position of labeled vesicles at the end of each sequence (supplementary movie 3, image every minute).

Figure 4

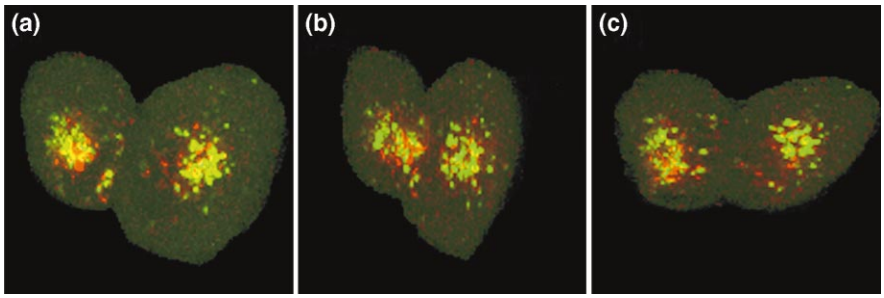

Three-dimensional reconstructions of newly formed daughter cells. MDCK cells expressing EEA1-GFP were incubated overnight with BSA-Alexa 594 and chased to label late endosomes and lysosomes. Cells were followed through mitosis with confocal microscopy, and five different z scans of newly formed daughter cells were acquired. The micrographs show three-dimensional representations of the data. **(a)** The z series merged to one plane. **(b)** The z series stack rotated vertically. **(c)** The z series stack rotated horizontally. (supplementary movie 4)

min or more and EEA1-GFP (Figure 3a). Data from such experiments showed that during mitosis, labeled vesicles were dispersed throughout the cytoplasm but accumulated at a juxtanuclear position right after cytokinesis (Figure 3a). This was facilitated by directional, coordinated movements (Figure 3b). In the merged version, there is seemingly an overlap between the two different labels (yellow in Figure 3a). However, as shown in Figure 4, three dimensional reconstitutions from the sections demonstrated that early and late endocytic compartments were also distinct and separate throughout cytokinesis (supplementary data available, movie 5). About 30 to 60 min after cytokinesis, endosomes and lysosomes started to migrate from the juxtanuclear position to distribute throughout the cytoplasm (Figure 3).

Endosomes and lysosomes are not accurately segregated to the daughter cells

The observed shift in the intracellular localization of the endocytic compartments during cell division suggested some degree of order to the partitioning of these organelles. To study if there was a higher degree of precision to the process than what would be expected by a random partitioning, the number of EEA1-GFP- or BSA-containing vesicles present after mitosis was estimated in the daughter cells and related to the number of labeled vesicles in the mother cell 30 min prior to mitosis. Data from analysis of 20 divisions were grouped, plotted, and related to the expected distribution of 100 endosomes partitioned by a random distribution (Figure 5).

The data show that the distribution of both early endosomes and late endocytic compartments was shifted slightly to the left of, but was not more focused than, the theoretical binomial distribution. From this, we may conclude that there is no strong mechanism assuring an equal distribution of the number of endosomal organelles to the two daughter cells. A shift to the left of the theoretical distributions is due to a lower number of labeled vesicles after mitosis. One explanation for this could be that 30 min after cytokinesis, the daughter cells were still in a rounded configuration, and it was therefore more difficult to identify separate vesicles. Three hours after cytokinesis, the daughter cells had flattened out, but on average, the number of labeled endosomes/lysosomes in the two daughter cells was only 90% of that of the parental cell before mitosis. At this time, the number of EEA1-GFP-labeled endosomes had increased to about 150% (data not shown), indicating that new early endosomes were formed in the early G1 phase.

Another explanation for the decreased number of vesicles in the daughter cells could be that some vesicles did fuse during mitosis. To address this possibility, cells were labeled overnight with BSA-Alexa 594 and chased for 30 min in microscope medium. The total BSA-Alexa 594 fluorescence within the mother cells was then quantified and related to the total fluorescence in the daughter cells (Figure 5). With this approach, we obtained a more narrow distribution than with the counted number of vesicles; however, the experimental data were still not within the borders of the calculated binomial distribution.

Enlarged endosomes are not fragmented during mitosis

Time-lapse fluorescence microscopy of labeled endosomes suggested that the endosomes and lysosomes did not fragment during mitosis. However, these observations did not rule out a possible transient fragmentation of the vesicles before cytokinesis, followed by rapid reassembly after cytokinesis. To study this in more detail, we utilized stably transfected MDCK cells with enlarged endosomes induced by high levels of invariant chain [11]. Growth experiments demonstrated that the generation time was only slightly prolonged in cells with enlarged endosomes (data not shown). Studies on fixed cells with enlarged endosomes and the DNA stained with ethidium bromide demonstrated that the enlarged endosomes were present in all mitotic phases (data not shown). Moreover, the size and stability of the enlarged endosomes allowed us to study the fate of single endosomes in dividing cells using time-lapse phase contrast microscopy. The results showed that the enlarged endosomes remained intact and were not detectably fragmented during mitosis and cytokinesis (Figure 6).

Figure 5

Quantitative analysis of endosome/lysosome partitioning. Images of mother cells 30 min before cytokinesis and daughter cells 30 min after division were analyzed digitally (see Materials and methods). The number of labeled endosomes and the value of total BSA-Alexa 594-labeling were determined, and the fractions found in the daughter cells were organized in groups and plotted. Data obtained from 17–23 time-lapse experiments are shown for each dataset. The random distribution was estimated by the binomial formula

$$P(r) = \left(\frac{N!}{r!(N-r)!}\right) p^r (1-p)^{N-r},$$

where $P(r)$ is the probability of exactly r successes. r (the probability for any endosome to be partitioned to any daughter cell) was set to 0.5, and, for simplicity reasons, N (the number of endosomes) was set to 100. The probabilities were then grouped and plotted.

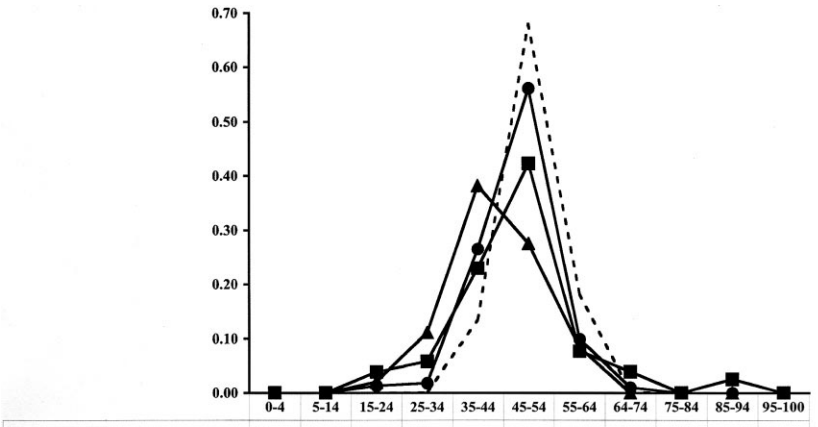

	0-4	5-14	15-24	25-34	35-44	45-54	55-64	64-74	75-84	85-94	95-100	Total
- - - - random	0.00	0.00	0.00	0.00	0.13	0.68	0.18	0.00	0.00	0.00	0.00	= 1.00
—■— EE 30	0.00	0.00	0.04	0.06	0.23	0.42	0.08	0.04	0.00	0.03	0.00	= 0.89
—▲— LE 30	0.00	0.00	0.02	0.11	0.38	0.28	0.08	0.00	0.00	0.00	0.00	= 0.84
—●— Total BSA-Alexa 594 labeling	0.00	0.00	0.01	0.02	0.27	0.56	0.10	0.01	0.00	0.00	0.00	= 0.91

Discussion and conclusion

In this paper, we have addressed two basic questions: are endosomes and lysosomes stable entities during mitosis, and, if so, how is the copy number maintained?; and are endosomes and lysosomes partitioned to the daughter cells in an ordered manner? To obtain the proper distribution of organelle membranes to the daughter cells, both the ER and the Golgi complex disassemble during mitosis. So far, the fate of endosomes during cell division has not been extensively studied. Due to extensive organelle movement and the small size of endosomes, following specific endosomal compartments during division and cytokinesis has been problematic.

To identify early endosomes, we used cells transfected with EEA1-GFP, and late endocytic compartments were identified by the uptake and chase of BSA-Alexa 594. By this method, we could clearly distinguish the two separate endosomal compartments in interphase cells with hardly any overlap of the two markers. As the cells assumed a rounded configuration during mitosis, the endosomal compartments became more clustered, but detailed three-dimensional analysis showed that, also in this phase, the markers did not significantly overlap. This shows that the endosomal compartments were separate throughout mitosis.

To study the fate of single endosomes during mitosis, we took advantage of the enlarged endosomes induced by Ii expression in stably transfected MDCK cells. Phase contrast video microscopy did not reveal detectable fragmentation of the enlarged endosomes during cell division. In addition, whereas fusion of endosomes could be readily observed in interphase cells (T.W.N, T.F.G., T.B., J.W., E.S., and O.B., unpublished data), this was not observed during mitosis. From the above data, we draw the conclusion that in MDCK cells, endosomes and lysosomes are maintained during cell division and do not fragment or fuse. This conclusion is also supported by previous data showing that the process of endocytosis is arrested upon

Figure 6

Phase contrast video microscopy of cells with invariant chain-induced enlarged endosomes. Formation of enlarged endosomes was induced by overnight expression of invariant chain, and phase contrast microscopy images of dividing, live cells at 37°C were acquired every minute for 4 hr. An asterisk identifies **(a)** the mother cell 60 min before division, **(b)** the mother cell during mitosis, and **(c)** the daughter cells 30 min after division (supplementary movie 6, image every minute).

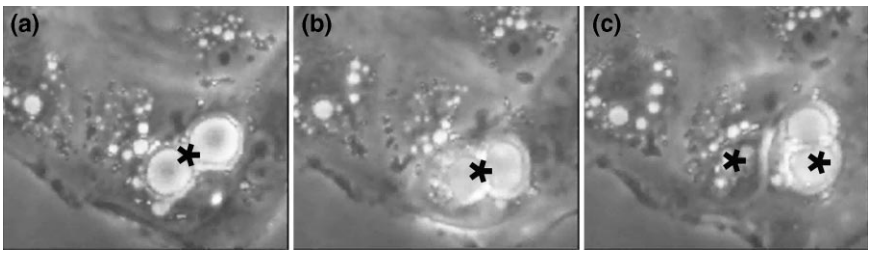

the entry into mitosis (for a review, see [12]) and data from cell-free systems showing that endosome fusion events are arrested in mitotic extracts [13, 14].

Endosomes and lysosomes have long been appreciated to be highly dynamic structures that exhibit microtubule-dependent, saltatory movements [15], a process facilitated by motor proteins (for a review, see [16]). Previous reports have shown that during mitosis, endosomes sometimes cluster at the mitotic spindle poles [17–20]. Our results show that after cytokinesis, early and late endocytic compartments inherited from the mother cell colocalized at a juxtanuclear position in the area of the microtubule organization center. Furthermore, immunofluorescence microscopy studies of fixed cells showed that these organelles colocalized with microtubules in all mitotic phases (data not shown). Together, these data hint at the possibility that microtubules play a role in endosome/lysosome partitioning, and we asked if this would cause endosomes and lysosomes to be partitioned with higher accuracy than by a random procedure. To address this question, we computer-analyzed a number of images from the time-lapse videos of dividing cells. The number of endosomes/lysosomes in mother and daughter cells were identified, and the fractions of labeled organelles were compared to the expected distribution of 100 endosomes partitioned by a random procedure. Partitioning of neither early endosomes nor late endosomes/lysosomes was within the expected distribution of 100 randomly segregated endosomes. Another method of studying the distribution of endosomal partitioning into daughter cells involves measuring the segregation of the fluorescent content of the mother cell endosomal compartments. This approach resulted in a more concentrated distribution, but not one that was more precise than would be expected by a stochastic mechanism, which would yield data that follows a binomial distribution. From our data, we find no evidence for a strict mechanism assuring an equal division of endosomes/lysosomes into the two daughter cells. A potential general size difference between daughter cells may also affect the distribution of these organelles. However, our results indicate that at least some part of the process of division of endosomes/lysosomes is stochastic.

The dispersed distribution does not rule out that there might be an order to the process. Our data show that during mitosis, the endosomal compartments are clustered by directional movements, suggesting that microtubules are involved in the process. It is possible that organelle association to either spindle is a stochastic process. Thus, although the spindle can serve as a track for precise segregation of its associated vehicles, endosomes/lysosomes would not be partitioned accurately if there was no mechanism to ensure that these organelles are bound in equal numbers to both forming spindles. Altogether, we may conclude that although organelle movement and colocalization analysis suggest that the segregation of endosomes and lysosomes might be ordered, the accuracy of partitioning is not higher than what would be expected by a stochastic distribution.

We found the cytoplasmic distribution of EEA1-GFP to increase upon the onset of mitosis. A similar pattern has been observed with rab4, which is phosphorylated during mitosis, causing the protein to redistribute to the cytoplasm [21–23]. EEA1 is recruited to early endosomal membranes by phosphatidyl inositol 3-phosphate [24–26], the SNARE syntaxin-6 [27], and the GTPase rab5 [28]. EEA1 plays an important role in endosome fusion [28–30] by acting as a tethering factor (for a review, see [31]). In a recent report, Nielsen et al. [32] have shown that rab5 both stimulates the association of early endosomes with microtubules and the movements of early endosomes toward the center of the cell. Interestingly, the rab5b isotype has been demonstrated to be phosphorylated by cdc2 kinase in vitro [33]. However, to our knowledge, the distribution of rab5b has not been studied during mitosis, and we can, at present, only speculate about a possible link between rab5 phosphorylation, the shift in EEA1 distribution, and the coordinated movement of endosomes during cytokinesis.

How then is the copy number of endosomes/lysosomes maintained as cells propagate? Our data show that the endosome/lysosome copy number was approximately halved after cell division. The number of early endosomes, which were labeled "biosynthetically" by EEA1-GFP, increased in the daughter cells after cell division (50% increase after 3 hr). This shows that the copy number of early endosomes increases in the daughter cells as endocytosis is reinitiated. However, the number of late endosomes containing endocytosed marker did not increase during the same period. As the number of late endosomes/lysosomes most likely also increases, the newly formed organelles do not seem to share the content of the lysosomes inherited from the mother cell. This could be a result of the "maturation" of the early endosomes into late endosomes and lysosomes. In conclusion, our data demonstrate that endosomes and lysosomes do not disintegrate during mitosis, but are partitioned as separate, intact vesicles. The partitioning is not accurate, and the copy number is increased after cytokinesis, which is most likely a direct result of the reinitiated endocytic machinery.

Materials and methods

Cells

Madin-Darby canine kidney strain II (MDCK) stably transfected with Ii under the control of the metallothionein promoter in the pMEP4 vector has been described previously [34]. Ii expression was induced by the addition of 25 μM $CdCl_2$. Cells were transfected with early endosomal antigen 1 fused to green fluorescent protein (EEA1-GFP) [35], a gift from Dr. H. Stenmark (Oslo, Norway). The cells were grown in complete medium: DMEM (Bio Whittaker) supplemented with 9% FCS (Integro),

2 mM glutamine, 25 U/ml penicillin, and 25 μg/ml streptomycin (all from Bio Whittaker) in 6% CO_2 in a 37°C incubator.

Immunofluorescence confocal and video microscopy

Stably transfected MDCK cells were grown in chambered coverglass (Nalgene) and incubated with DMEM/0.15 μg/ml bovine serum albumin (BSA) conjugated to BSA-Alexa 594 (Molecular Probes) overnight. Cells were then washed and incubated further with microscopy medium (DMEM without phenol red and sodium bicarbonate, supplemented with 3,5 g/L D-glucose monohydrate to a final concentration of 4,5 g/L; 25 mM HEPES, adjusted to pH 8 with NaOH; and FCS added to 9%) for at least 30 min before microscopy sessions were started. A constant temperature of 37°C was obtained by a fan controlled by a sensor embedded in the chamber medium.

Confocal images were acquired with a Leica DM IRBE inverted microscope stand (Leica) equipped with a Leica 40/0.7 air objective, a TCS-NT digital scanning head, and an Ocra 100 C4742–95 CCD camera (Hamamatshu Photonics). For confocal imaging, GFP molecules and BSA-Alexa 488 were excited with the 488 line of a krypton-argon laser and imaged with 515–540 band-pass filters. BSA-Alexa 594 Red were excited with the 568 line and imaged with long-pass 590 filters. The digital camera was connected to an Apple Power Macintosh 9600/300 (Apple) equipped with a PCI-based Snapper DIG 16 video grabbing card. Video data acquisition and three-dimensional modeling were performed using Openlab (Improvision). Quick Time (Apple) video presentations were edited with EditDV (Digital Origin) and compressed using Cinepak (Apple) or Sorensen Developer 2.1 (Sorenesen Viscion) codecs. Photoshop (Adobe Systems) was used for image processing and presentation.

Quantitative immunofluorescence microscopy

Quantitative analysis of selected images obtained from the time-lapse experiments was performed on a Macintosh Power PC (Apple) using density slicing, advanced measurements, and automation modules of OpenLab. First, five confocal images from different z levels of the same cells were merged. For quantification of the number of labeled organelles, background noise was subtracted. The cell boundaries were then identified on reflective light images and used to define the region of interest (ROI). Next, binary image files were made, displaying all pixels in the 100–255 range of 8-bit grayscale images of each ROI, corresponding to the bright signals on the fluorescence images. The binary files were then used to calculate the number of clusters larger than four pixels that were not touching the edge of the ROI.

In principle, the total cell labeling was quantified by a similar method, but in this case, separate binary files were made for each pixel intensity in the range 100–255. The number of pixels of each of the resulting 156 binary files was multiplied by the corresponding pixel intensity, e.g., the number of pixels with an intensity of 100 was multiplied by 100, the number of pixels with an intensity of 101 was multiplied by 101, and so on. The total specific fluorescence of each ROI was finally calculated as the sum of all relevant pixels, multiplied by their corresponding intensity.

Materials

All materials, unless specified otherwise, were purchased from Sigma.

Supplementary material

The data presented in this article were originally acquired as image sequences from which a selection has been displayed in the figures. More information about the partitioning of endosomes during mitosis can be found in the supplementary materials in the form of six movies at http://images.cellpress.com/supmat/supmatin.htm.

Acknowledgements

We would like to thank Bjørn Langrekken for building the microscope temperature regulation device and Arne Løvlie, Stéphane Méresse, and Harald Stenmark for helpful discussions. This work was supported by the Norwegian Cancer Society, the Norwegian Research Council, and Novo Nordisk Fonden.

References

1. McIntosh JR, Koonce MP: **Mitosis**. *Science* 1989, **246:**622-628.
2. Birky CW Jr: **The partitioning of cytoplasmic organelles at cell division.** *Int Rev Cytol Suppl* 1983, **15:**49-89.
3. Nelson WJ: **W(h)ither the Golgi during mitosis?** *J Cell Biol* 2000, **149:**243-248.
4. Shima DT, Haldar K, Pepperkok R, Watson R, Warren G: **Partitioning of the Golgi apparatus during mitosis in living HeLa cells.** *J Cell Biol* 1997, **137:**1211-1228.
5. Shima DT, Cabrera-Poch N, Pepperkok R, Warren G: **An ordered inheritance strategy for the Golgi apparatus: visualization of mitotic disassembly reveals a role for the mitotic spindle.** *J Cell Biol* 1998, **141:**955-966.
6. Hopkins CR, Gibson A, Shipman M, Miller K: **Movement of internalized ligand-receptor complexes along a continuous endosomal reticulum.** *Nature* 1990, **346:**335-339.
7. Tooze J, Hollinshead M: **Tubular early endosomal networks in AtT20 and other cells.** *J Cell Biol* 1991, **115:**635-653.
8. Steinman RM, Silver JM, Cohn ZA: **Pinocytosis in fibroblasts. Quantitative studies in vitro.** *J Cell Biol* 1974, **63:**949-969.
9. Steinman RM, Brodie SE, Cohn ZA: **Membrane flow during pinocytosis. A stereologic analysis.** *J Cell Biol* 1976, **68:**665-687.
10. Weisman LS, Bacallao R, Wickner W: **Multiple methods of visualizing the yeast vacuole permit evaluation of its morphology and inheritance during the cell cycle.** *J Cell Biol* 1987, **105:**1539-1547.
11. Stang E, Bakke O: **MHC class II associated invariant chain induced enlarged endosomal structures. A morphological study.** *Exp Cell Res* 1997, **235:**79-82.
12. Warren G: **Membrane partitioning during cell division.** *Annu Rev Biochem* 1993, **62:**323-348.
13. Tuomikoski T, Felix MA, Doree M, Gruenberg J: **Inhibition of endocytic vesicle fusion in vitro by the cell-cycle control protein kinase cdc2.** *Nature* 1989, **342:**942-945.
14. Thomas L, Clarke PR, Pagano M, Gruenberg J: **Inhibition of membrane fusion in vitro via cyclin B but not cyclin A.** *J Biol Chem* 1992, **267:**6183-6187.
15. Herman B, Albertini DF: **A time-lapse video image intensification analysis of cytoplasmic organelle movements during endosome translocation.** *J Cell Biol* 1984, **98:**565-576.
16. Goodson HV, Valetti C, Kreis TE: **Motors and membrane traffic.** *Curr Opin Cell Biol* 1997, **9:**18-28.
17. Zeligs JD, Wollman SH: **Mitosis in rat thyroid epithelial cells in vivo. I. Ultrastructural changes in cytoplasmic organelles during the mitotic cycle.** *J Ultrastruct Res* 1979, **66:**53-77.
18. Tamaki H, Yamashina S: **Changes in cell polarity during mitosis in rat parotid acinar cells.** *J Histochem Cytochem* 1991, **39:**1077-1087.
19. Kaplan KB, Swedlow JR, Varmus HE, Morgan DO: **Association of p60c-src with endosomal membranes in mammalian fibroblasts.** *J Cell Biol* 1992, **118:**321-333.
20. Tooze J, Hollinshead M: **In AtT20 and HeLa cells brefeldin A induces the fusion of tubular endosomes and changes their distribution and some of their endocytic properties.** *J Cell Biol* 1992, **118:**813-830.
21. Bailly E, McCaffrey M, Touchot N, Zahraoui A, Goud B, Bornens M: **Phosphorylation of two small GTP-binding proteins of the Rab family by p34cdc2.** *Nature* 1991, **350:**715-718.
22. van der Sluijs P, Hull M, Huber LA, Male P, Goud B, Mellman I: **Reversible phosphorylation–dephosphorylation determines the localization of rab4 during the cell cycle.** *EMBO J* 1992, **11:**4379-4389.
23. Ayad N, Hull M, Mellman I: **Mitotic phosphorylation of rab4 prevents binding to a specific receptor on endosome membranes.** *EMBO J* 1997, **16:**4497-4507.
24. Patki V, Virbasius J, Lane WS, Toh BH, Shpetner HS, Corvera S: **Identification of an early endosomal protein regulated by phosphatidylinositol 3-kinase.** *Proc Natl Acad Sci USA* 1997, **94:**7326-7330.
25. Gaullier JM, Simonsen A, D'Arrigo A, Bremnes B, Stenmark H, Aasland R: **FYVE fingers bind Ptdins(3)P.** *Nature* 1998, **394:**432-433.
26. Burd CG, Emr SD: **Phosphatidylinositol(3)-phosphate signaling mediated by specific binding to RING FYVE domains.** *Mol Cell* 1998, **2:**157-162.
27. Simonsen A, Gaullier JM, D'Arrigo A, Stenmark H: **The Rab5**

effector EEA1 interacts directly with syntaxin-6. *J Biol Chem* 1999, **274:**28857-28860.
28. Simonsen A, Lippé R, Christoforidis S, Gaullier JM, Brech A, Callaghan J, *et al.*: **EEA1 links PI(3)K function to Rab5 regulation of endosome fusion.** *Nature* 1998, **394:**494-498.
29. Mills IG, Jones AT, Clague MJ: **Involvement of the endosomal autoantigen EEA1 in homotypic fusion of early endosomes.** *Curr Biol* 1998, **8:**881-884.
30. Christoforidis S, McBride HM, Burgoyne RD, Zerial M: **The Rab5 effector EEA1 is a core component of endosome docking.** *Nature* 1999, **397:**621-625.
31. Waters MG, Pfeffer SR: **Membrane tethering in intracellular transport.** *Curr Opin Cell Biol* 1999, **11:**453-459.
32. Nielsen E, Severin F, Backer JM, Hyman AA, Zerial M: **Rab5 regulates motility of early endosomes on microtubules.** *Nat Cell Biol* 1999, **1:**376-382.
33. Chiariello M, Bruni CB, Bucci C: **The small GTPases Rab5a, Rab5b and Rab5c are differentially phosphorylated in vitro.** *FEBS Lett* 1999, **453:**20-24.
34. Nordeng TW, Bakke O: **Overexpression of proteins containing tyrosine- or leucine-based sorting signals affects transferrin receptor trafficking.** *J Biol Chem* 1999, **274:**21139-21148.
35. McBride HM, Rybin V, Murphy C, Giner A, Teasdale R, Zerial M: **Oligomeric complexes link Rab5 effectors with NSF and drive membrane fusion via interactions between EEA1 and syntaxin 13.** *Cell* 1999, **98:**377-386.